

Real-time monitoring of all-optical poling by two-beam second-harmonic generation

Arri Priimagi

Department of Engineering Physics and Mathematics and Center for New Materials,
Helsinki University of Technology, P.O. Box 2200, FI-02015 HUT, Espoo, Finland

Stefano Cattaneo* and Martti Kauranen

Institute of Physics, Tampere University of Technology, P.O. Box 692, FI-33101 Tampere, Finland

Received March 6, 2006; accepted April 27, 2006; posted May 2, 2006 (Doc. ID 68713)

We demonstrate a simple method for monitoring all-optical poling in real time. The poling pattern created by the writing beam at the fundamental frequency and the seed beam at the second-harmonic frequency is reconstructed by two-beam second-harmonic generation because of the writing beam and an additional probe beam at the fundamental frequency. When the probe beam is sufficiently weak, it does not distort the poling process. The method provides a significantly stronger signal than monitoring based on a probe beam alone. © 2006 Optical Society of America

OCIS codes: 190.2620, 160.5470, 350.2770.

Since the observation of a light-induced second-harmonic generation in optical fibers,^{1,2} many efforts have been made to break the centrosymmetry of isotropic materials by purely optical means. The demonstration of all-optical poling in organic polymer-based materials³ has opened up an alternative way to orient the active moieties in a polymer matrix, resulting in nonlinearities comparable to those reached by electric-field poling.⁴ Unlike electric-field poling, all-optical poling can be extended beyond dipolar molecules,⁵ and allows controlling the symmetry properties of the photoinduced susceptibility by properly choosing the polarizations of the writing beams.⁶

All-optical poling is performed by irradiating a sample with a coherent superposition of two beams, one at the fundamental (writing beam) and one at the second-harmonic (seeding beam) frequency.⁷ The nonzero temporal average of the cube of the total field results in a second-order susceptibility pattern to be recorded in the medium, which can be reconstructed (i.e., used for second-harmonic generation) by irradiating the sample with a beam at the fundamental frequency. The process is typically implemented by using a collinear measurement geometry and by alternating the writing and reading sequences. However, frequent interruption of the writing process distorts the poling dynamics,⁸ which has led to efforts toward monitoring the evolution of the signal in real time.

Previous real-time monitoring methods have employed the same fundamental beam for both recording and reconstruction. Churikov *et al.*⁸ exploited the different polarization behavior of the seeding and signal beams: When the polarizations of the writing and seeding beams are not parallel or perpendicular, the seeding and signal beams have different linear polarizations, allowing real-time monitoring of the signal. This, however, limits the possible combinations of input polarizations and, consequently, the symmetry properties of the photoinduced susceptibility

pattern.⁶ Apostoluk *et al.*⁹ have, in turn, shown that when the sample is placed on a glass prism, the material dispersion results in a phase-independent poling process that can be monitored in real time because of the presence of a weak beam propagating noncollinearly with the seeding beam.

In this Letter, we demonstrate a particularly simple means for real-time monitoring of all-optical poling. The technique is based on a two-beam second-harmonic generation between the fundamental writing beam and a noncollinear probe beam at the fundamental frequency. Such a second-harmonic signal is spatially separated from the seeding beam, and therefore can be easily detected. We show both by experiment and by simple phase-matching considerations that when the probe beam is sufficiently weak, the additional gratings formed because of the presence of the probe beam do not disturb the recording process, and the joint second-harmonic signal depicts the $\chi^{(2)}$ susceptibility grating recorded by the collinear writing and seeding beams. An important advantage is that the process is partly driven by the strong fundamental writing beam, resulting in a stronger monitoring signal than, e.g., in Ref. 9.

The experimental setup is presented in Fig. 1. As a light source, we used a Q-switched flashlamp pumped Nd:YAG laser delivering 10 ns pulses at the

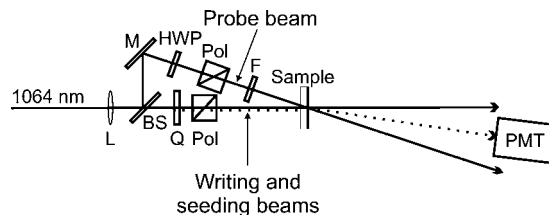


Fig. 1. Schematic of the experimental setup. Abbreviations: L, 50 cm lens; BS, beam splitter; Q, quartz crystal for generating the seeding beam; M, mirror; HWP, half-wave plate; Pol, polarizer; F, IR pass filter; PMT, photomultiplier tube.

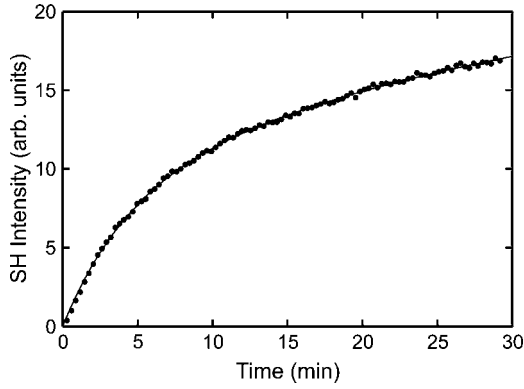


Fig. 2. Real-time growth dynamics of the all-optical poling signal. The fitting function is of the form $f(t)=A_1[1-\exp(-t/\tau_1)]+A_2[1-\exp(-t/\tau_2)]$.

repetition rate of 30 Hz. The fundamental beam was focused weakly with a 50 cm lens and split into two beams with a pulse energy of approximately 8.3 mJ. The energy of the probe beam was controlled with a half-wave plate–polarizer combination, and second-harmonic light produced by the optical components was filtered out before reaching the sample. The writing and probe beams were applied on the same spot on the sample, with incident angles of 0° and 15° , respectively. A weak second-harmonic seeding beam was generated in a thin quartz crystal and was collinear with the fundamental writing beam. All beams were p polarized. The second-harmonic signal was monitored with a photomultiplier tube in a direction determined by the sum of the wave vectors of the two fundamental beams.

As a sample, we used a guest–host system of 10 wt. % Disperse Red 1 doped in poly(methyl methacrylate), which has been shown to produce an efficient all-optical poling signal even with low-seeding intensity.⁸ Hence the optimization of the relative intensities of the writing and seeding beams was not required. The film was prepared by spin coating (60 s, 5000 rpm) a 10 wt. % solution of the constituents in tetrahydrofuran onto a glass substrate. The sample thickness was approximately $1.2 \mu\text{m}$, and the optical density at 532 nm was 0.74.

A typical growth dynamics of the second-harmonic signal with a biexponential fit is illustrated in Fig. 2. The origin of the signal can be understood by considering the second-order susceptibility gratings formed in the sample in more detail. We take the writing and seeding beams to be plane waves of the form $E_\omega = A_\omega \exp(i\mathbf{k}_\omega \cdot \mathbf{r})$ and $E_{2\omega} = A_{2\omega} \exp(i\mathbf{k}_{2\omega} \cdot \mathbf{r})$, respectively. The induced susceptibility pattern is proportional to⁷

$$\chi^{(2)} \propto (A_\omega^2)^* A_{2\omega} \exp(i\Delta\mathbf{k}_1 \cdot \mathbf{r}) + \text{c.c.}, \quad (1)$$

where $\Delta\mathbf{k}_1 = \mathbf{k}_{2\omega} - 2\mathbf{k}_\omega$ is the wave-vector mismatch. If the pattern formed by the collinear beams is reconstructed with the combination of the writing beam E_ω and the probe beam E'_ω (see Fig. 1), the resulting second-order polarization is $P_{2\omega} \propto \chi^{(2)} E_\omega E'_\omega$. This yields

$$P_{2\omega} = (A_\omega^2)^* A_\omega A'_\omega A_{2\omega} \exp[i(\Delta\mathbf{k}_1 + \mathbf{k}_\omega + \mathbf{k}'_\omega) \cdot \mathbf{r}] + A_\omega^3 A'_\omega A_{2\omega}^* \exp[i(-\Delta\mathbf{k}_1 + \mathbf{k}_\omega + \mathbf{k}'_\omega) \cdot \mathbf{r}]. \quad (2)$$

The second-harmonic monitoring signal generated in the sum direction can be expressed as $E_{\text{SHG}} = A_{\text{SHG}} \exp(i\mathbf{k}_{\text{SHG}} \cdot \mathbf{r})$, where $\mathbf{k}_{\text{SHG}} = \mathbf{k}_\omega + \mathbf{k}'_\omega + \Delta\mathbf{k}_2$. The phase mismatches for the first and second terms in Eq. (2) are then $\Delta\mathbf{k}_2 - \Delta\mathbf{k}_1$ and $\Delta\mathbf{k}_2 + \Delta\mathbf{k}_1$, respectively. Note that for small angles between the two fundamental beams, $\Delta\mathbf{k}_1$ and $\Delta\mathbf{k}_2$ are nearly parallel and have the same sign and almost the same magnitude. Thus if the sample thickness is comparable to the coherence length $\pi/\Delta k_1$, we expect the first term to dominate.

In addition to the case described above, other susceptibility gratings, formed due to the interactions between the probe and the seed beam and between all three beams, need to be considered. The grating, as a result of the interaction between the probe beam and the seed beam, does not contribute to the signal in the sum direction $\mathbf{k}_\omega + \mathbf{k}'_\omega$. The grating written by all three beams produces two terms with potential influence:

$$P_{2\omega,1} = A_\omega^3 A'_\omega A_{2\omega}^* \exp[i(-\Delta\mathbf{k}_1 + \mathbf{k}_\omega + \mathbf{k}'_\omega) \cdot \mathbf{r}], \quad (3)$$

$$P_{2\omega,2} = A_\omega^* (A'_\omega)^2 (A_\omega)^* A_{2\omega} \exp[i(\Delta\mathbf{k}_1 + \mathbf{k}_\omega + \mathbf{k}'_\omega) \cdot \mathbf{r}]. \quad (4)$$

For the former, which is reconstructed by the writing beam, the phase mismatch is $\Delta\mathbf{k}_2 + \Delta\mathbf{k}_1$. This contribution is, therefore, expected to be negligible by the same reasoning used in the context of the second term in Eq. (2). For the term of Eq. (4), on the other hand, the phase mismatch is $\Delta\mathbf{k}_2 - \Delta\mathbf{k}_1$. However, the pattern is reconstructed by the probe beam and scales cubically with its amplitude. Thus we expect the term to be significant only when using a strong probe beam.

To study the influence of the probe beam on the poling signal, we compared the evolution of the signal when the probe beam was incident on the sample during the whole measurement and when it was applied on the sample for a short time at 3 min intervals. The saturation curves for a weak probe ($I_\omega/I'_\omega \sim 750$) are presented in Fig. 3a. The curves are measured from different points on the sample and are normalized to eliminate point-to-point variations in the signal level due to sample inhomogeneities. The poling dynamics is observed to be identical in both cases. In addition, when the probe beam was left on after approximately 25 min of poling, the evolution of the signal was unaffected. We also observed that if either of the fundamental beams was blocked after 30 min of poling, the signal vanished instantaneously. This indicates that both beams are required for the reconstruction process and excludes the possibility of linear scattering of the seed beam from any of the gratings into the detector.

For a strong probe ($I_\omega/I'_\omega \sim 5$), the evolution of the signal differs dramatically for the two cases, as can be seen from Fig. 3b. Most of all, when the probe was left on after approximately 25 min of poling, we ob-

served a biexponential decay in the poling signal, which indicates that the competing gratings formed in the sample perturb the poling performed by the two collinear beams. Profound understanding of this result requires a more detailed characterization of the different gratings formed in the sample, because when the writing and probe beams are of comparable intensity, the holographic nature of the noncollinear all-optical poling is unfolded.¹⁰ However, the signal still vanished instantaneously when blocking either of the fundamental beams, suggesting that the gratings presented in Eqs. (3) and (4) still do not contribute to the signal in the sum direction. The decay could also be due to photostimulated relaxation of the polar orientation of the dye molecules caused by the intense probe beam.¹¹ In any case, we conclude that to obtain nondestructive real-time monitoring of the collinear poling process, the probe intensity must be

very low compared with the writing beam intensity. This can be carried out without fully sacrificing the overall signal level, because two-beam second-harmonic generation scales linearly with the probe intensity, whereas monitoring only with a weak probe beam would scale quadratically.

In conclusion, we have demonstrated that all-optical poling in polymer samples can be monitored in real time by reconstructing the susceptibility pattern with two-beam second-harmonic generation based on the interaction between the fundamental writing beam and a weak fundamental probe beam. The additional gratings formed as a result of the presence of the probe beam do not contribute to the signal, provided that the probe is sufficiently weak. The demonstrated method significantly facilitates the experimental setup required for real-time monitoring of all-optical poling and is applicable to samples of different types.

We acknowledge the financial support from the National Technology Agency of Finland. We also acknowledge the support and conversations of O. Ikkala and M. Kaivola and the technical assistance of F. Rodriguez. A. Priimagi's e-mail address is arri.priimagi@tkk.fi.

*Present address: Philips Research, High Tech Campus 34, 5656 AE Eindhoven, The Netherlands.

References

1. U. Österberg and W. Margulis, *Opt. Lett.* **11**, 516 (1986).
2. R. H. Stolen and H. W. K. Tom, *Opt. Lett.* **12**, 585 (1987).
3. F. Charra, F. Kajzar, J. M. Nunzi, P. Raimond, and E. Idiart, *Opt. Lett.* **18**, 941 (1993).
4. C. Fiorini, F. Charra, J. M. Nunzi, and P. Raimond, *Nonlinear Opt.* **9**, 339 (1995).
5. C. Fiorini, F. Charra, J. M. Nunzi, I. D. W. Samuel, and J. Zyss, *Opt. Lett.* **20**, 2469 (1995).
6. S. Brasselet and J. Zyss, *Opt. Lett.* **22**, 1464 (1997).
7. N. B. Baranova and B. Ya. Zel'dovich, *J. Opt. Soc. Am. B* **8**, 27 (1991).
8. V. M. Churikov, M. F. Hung, and C. C. Hsu, *Opt. Lett.* **25**, 960 (2000).
9. A. Apostoluk, D. Chapron, G. Gadret, B. Sahraoui, J. M. Nunzi, C. Fiorini-Debuisschert, and P. Raimond, *Opt. Lett.* **27**, 2028 (2002).
10. N. Tsutsumi and T. Shingu, *Chem. Phys. Lett.* **403**, 420 (2005).
11. C. Fiorini, F. Charra, J. M. Nunzi, and P. Raimond, *J. Opt. Soc. Am. B* **14**, 1984 (1997).

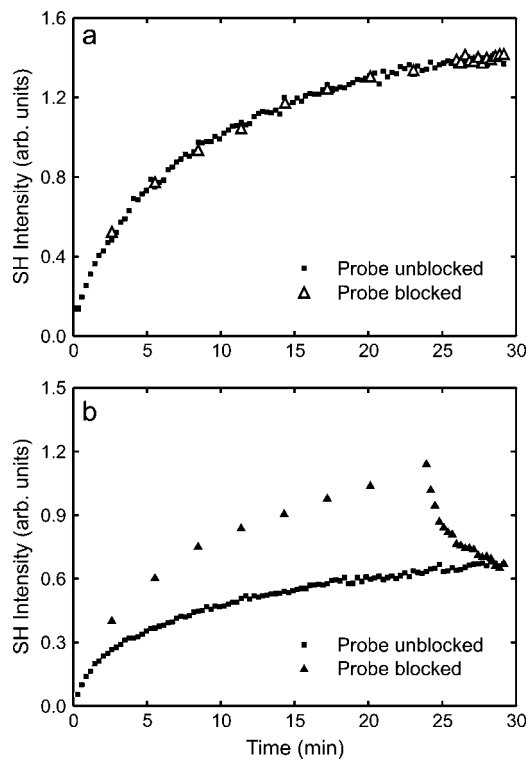


Fig. 3. Comparison of the poling dynamics for a, weak probe and b, strong probe when the probe beam is applied on the sample during the whole measurement (squares) and when it is applied for a short time at 3 min intervals to obtain measurement points (triangles). The curves are normalized to eliminate the point-to-point variations in the signal level due to sample inhomogeneities.